Microchemical Journal 128 (2016) 297–304

Contents lists available at ScienceDirect

Microchemical Journal

journal homepage: www.elsevier.com/locate/microc

Nano-supramolecular complex synthesis: Switch on/off enhanced fluorescence control and molecular release using a simple chemistry reaction

A. Guillermo Bracamonte [a,*], Danny Brouard [b], Mathieu Lessard-Viger [b], Denis Boudreau [b,*], Alicia V. Veglia [a]

[a] Instituto de Investigaciones en Fisicoquímica de Córdoba (INFIQC), Departamento de Química Orgánica, Facultad de Ciencias Químicas, Universidad Nacional de Córdoba, Ciudad Universitaria, 5000 Córdoba, Argentina
[b] Departement de chimie and Centre d'optique, photonique et laser (COPL), Université Laval, Québec G1V 0A6, QC, Canada

ARTICLE INFO

Article history:
Received 10 March 2016
Received in revised form 14 May 2016
Accepted 16 May 2016
Available online 18 May 2016

Keywords:
β-Cyclodextrin
Gold nanoparticles
Metal-enhanced fluorescence
Switch on/off control

ABSTRACT

A nanosensor based on β-cyclodextrin (βCD) macrocycles linked to gold nanoparticles for rhodamine B (RhB) sensing was developed applying the metal-enhanced fluorescence effect (MEF). Hence, we have developed many ways to control the distance of supramolecular systems to nanoparticle surface with different bioconjugation strategies in order to optimize signal detection. Different PEG spacer arm lengths were used to cover the nanoparticle surface with molecular spacers. This type of molecular shell is biocompatible, enabling to switch on/off the MEF effect using a dithiane linker by a simple reduction reaction. In the presence of the nanosensor obtained, an increase was observed in RhB fluorescence emission depending on molecular length, that is a characteristic effect of MEF. The major increase measured was 60% compared with RhB emission in buffer at 1 nM level, for a spacer length of 3.58 nm and an 80% increase as compared with that in the presence of βCD. These differences are ascribed to the fact that, in the presence of macrocycle, we can observe a well-known quenching effect that is overcome by the presence of the metallic core. Even at shorter spacer distances, with PEG lengths of 1.2 and 2.17 nm, increases of 25 and 47% respectively allow the analyte detection by the RhB complexation with βCD. The optimal MEF enhancement was measured with the maximal emission signal stabilized after 50 min due to plasmonic effects based on inter nanoparticle interactions. Moreover, the emission increase, in the presence of the metallic core, was accompanied with a diminution in the fluorescence lifetime's decay value averages, characteristic of MEF. This fact shows that the excited state is protected from the non-radiative emission decays enhancing the analytical signal.

1. Introduction

For the bionanosensor design, we needed to take into account two major parameters: the signal detection recorded; and the recognition system that would allow detecting the target. In the last years, supramolecular chemistry showed many examples developed from dye recognition and quantification using receptors [1]. The most well-known macrocycles in supramolecular chemistry are calixarenes [2] (CA), cucurbiturils [3] (CB) and cyclodextrins [4] (CD). All these receptors have a nanocavity with different organic groups that can interact with the guest included.

In this work we studied the use of cyclodextrins as a recognition supramolecular system, joined to gold nanoparticles for nanosensor developments based on metal enhanced fluorescence (MEF).

Cyclodextrins (CDs) are cyclic oligosaccharides consisting of six (αCD), seven (ßCD) or eight (γCD) units of α-D-glucose linked by α-(1,4) bonds. These macrocycles have a nanocavity (internal diameter of 0.7 nm for βCD) which allows them to act as hosts to form inclusion complexes with guest molecules in the solid state or in solution. CDs are interesting microvessels capable of embedding appropriately sized molecules, and the resulting supramolecules can serve as excellent miniature models for enzyme–substrate complexes.

Moreover it is well known that rhodamine B (RhB) interacts strongly with βCD [5,6]. For this reason, and looking for a good target model to evaluate our nano-supramolecular system, we worked with this dye. RhB is an important xanthene dye with a large variety of technical applications, including dye lasers, photosensitizer and quantum counter [7]. The spectroscopic and photophysical properties of RhB have already been extensively studied in different media. Recently, Jian Zhu et al. have studied the mechanisms of interaction between bovine serum albumin nanoparticles with RhB loaded using fluorescence spectroscopy in order to design a drug delivery system [8].

* Corresponding authors.
E-mail addresses: gbracamonte@fcq.unc.edu.ar (A.G. Bracamonte), denis.boudreau@chm.ulaval.ca (D. Boudreau).

http://dx.doi.org/10.1016/j.microc.2016.05.009
0026-265X/

Metal enhanced fluorescence (MEF) is a plasmonic effect that enhances the emission fluorescence of a substrate placed at a given distance from a metallic surface [9].

The MEF effect depends of the distance of the fluorophore from the metallic surface because the electromagnetic field intensity decays exponentially ($1/r^3$) affecting drastically the fluorophore excitation [10]. For this reason in order to evaluate this parameter there are many studies developed using polymeric spacers such as silica [11]. In these nanoarchitectures, the fluorophore is covalently bonded and the concentration can be controlled for maximal enhancements. These studies are in progress over surfaces [12] and colloidal dispersions [13], depending on the nanoarchitecture design and applications.

In nanosensor developments, there are many studies done with surfaces chemically modified with molecular spacer appending different supramolecular receptors at different distances by different instrumental techniques. But as far as we know there is no reported nanosensor with molecular spacers, based on an on/off MEF switch.

The following examples about molecular spacers used to modify nanoparticle surfaces with cyclodextrins as part of nanosensors coupled with many analytical methodologies could be mentioned. Campina et al. reported gold electrodes modified with 11-amino-1-undecanethiol and di-(N-succinimidyl) carbonate for βCD linking [14]. With this surface modification it was possible to shift the oxidation peak at higher potentials compared with those of the free gold surface, showing a good correlation response of hydroquinone with dopamine. A further example involves the fluorescent method developed by Zhang N. et al., based on a novel assembly of gold nanoparticles grafted with βCD monothiolated for the fluorescent probing of cholesterol, using a Förster Resonance Energy Transfer (FRET) control strategy [15]. Another recent case is a quantitative colorimetric method developed using silver nanoparticles modified with thiolated βCD, for organic isomer discrimination [16]. In most design strategies, the use of monothiolated cyclodextrins directly grafted over nanoparticle surfaces was reported. Yet, other studies, including those conducted by Wu et al., were designed with molecular spacers. It was synthesized magnetic nanoparticles grafted with amine-β-cyclodextrin via a novel synthetic route using poly(ethylene glycol) PEG activated as linkers. These nanoparticles were used for dopamine electrochemical detection [17]. The surface properties of magnetic nanoparticles with PEG spacer arms linked were also studied by isothermal titration calorimetry and dynamic light scattering (DLS) methods [18]. Enthalpy–entropy analysis suggested that poly(ethylene glycol) (PEG) modification on particle surface could effectively reduce the interaction between magnetic nanoparticles and plasma proteins, showing that the use of this type of linkers is a particularly good choice for nanosensors likely to be applied to biological media.

In all the examples mentioned, the cyclodextrin cavities were used as efficient dye recognition nanocavities and signal modifiers for sensor developments. But, also it is important to mention about the application of CDs in pharmaceutics and nanomedicine. For example the first experimental therapeutic application with cyclodextrin self-assemblies was developed and applied in humans to provide targeted delivery of RNA [19]. By similar manner, novel quaternary ammonium β-cyclodextrin (QAβCD) nanoparticles as drug delivery carriers for doxorubicin (DOX), a hydrophobic anticancer drug, across the blood brain barrierwere developed [20]. For this reason, from the drug delivery point of view, the design and synthesis of new prototypes of supramolecular nanoparticles applied in nanomedicine is also of high interest.

The final goal of this work was to join the supramolecular knowledge to metallic nanoparticles for a nanosensor design based on MEF for nanoimaging and new analytical methodology developments [21]. For this reason, the study of different ways to control the distance of the supramolecular system to the nanoparticle surface with different bioconjugation strategies was required to optimize the effect needed depending on the application. Different PEG spacer arm lengths were used to cover the nanoparticle surface, thus it is possible to switch on/off the metal-enhanced fluorescence effect (MEF) using a dithiane linker by a simple reduction reaction. These PEG molecular shells are biocompatible and prevent aggregation in cellular media.

2. Experimental

2.1. Apparatus

UV–vis and spectrofluorimetric determinations were carried out in a Varian UV-50 Carry 50 Conc. and a Fluorolog HORIBA JOBIN YVON, respectively. Lifetime measurements were done with a PicoQuant, Fluotime 2000. The pH was measured with a Fisher Scientific Accumet model Excel XL20 at 25.0 ± 0.1 °C. The pH-meter was first calibrated using standard buffers (pH = 4.00; 7.00; and 9.00). An ultrasonic bath (Branson 2510) was used for the dispersion of the reagents. Transmission electron microscopy (TEM) images were taken using a TEM JEM-1230, JEOL with an operating voltage of 200 kV. Data analysis was performed with Origin (Scientific Graph system) version 8.

2.2. Reagents

Water was obtained using a Millipore apparatus. RhB (99% purity, Sigma-Aldrich), βCD (98% purity, Sigma), hydrogen tetrachloroaurate, $HAuCl_4 \cdot 3H_2O$ (99%, Sigma-Aldrich), citrate sodium tribasic dehydrate (99%, ACS reagent), polyvinyl pyrrolidone 40,000 g/mol (98%, Sigma-Aldrich) and mercaptophenylboronic acid (≥95%, Aldrich) were used as received. The spacer arms 3,3′-dithiobis(sulfosuccinimidyl)propionate (DTSSP), and bis-succinimide ester activated PEG (polyethylene glycol) compounds for crosslinking $BS(PEG)_n$ were from Fisher Scientific company. The pH = 7.4 (10 mM) buffer was prepared according to literature procedures (2.3 mM monosodium dihydrogen phosphate and disodium hydrogen phosphate 7.7 mM). All buffer constituents were commercial analytical-grade reagents.

2.3. General procedure

Gold nanoparticles were synthesized by the classical Turkevich method of citrate reduction of $HAuCl_4$ and were afterward stabilized with PVP 40. The resulting nanoparticles were then redispersed in anhydrous ethanol (mother solution, [Au NPs] = $3.88.10^{10}$ NPs/mL, diameter = 55.5 nm). This nanoparticle diameter was chosen in order to get an optimal nanoparticle plasmon band to interact with the fluorophore.

After that the surface of the nanoparticles was modified with 3-(aminopropyl)triethoxysilane (APS) to functionalize it with amine groups. Over this surface different spacer lengths of bis-succinimide ester activated PEG (polyethylene glycol) compounds (BS(PEG)) were covalently bonded by stable amide bonds. The spacer arms used were with $n = 5$ (BS $(PEG)_5$, 2.17 nm) and $n = 9$ (BS $(PEG)_9$, 3.58 nm). Moreover, we chose a cross-linker with disulfide bonds for cyclodextrin–rhodamine B complex delivery, with 1.2 nm spacer length, called 3,3′-dithiobis(sulfosuccinimidyl)propionate (DTSSP). After DTSSP cyclodextrin linking, we were able to reduce the disulfide covalent bond with a specific reducing agent, DL-1,4-dithiothreitol (DTT) for complex delivery. In general, we called the nanoparticles βCD grafted with different spacers as Au@$spacer_n$-βCD.

For 5 mL of gold nanoparticles in ethanol, 50 μL of APS was added and allowed to react for 2 h at room temperature. Nanoparticles were centrifugated and washed with ethanol. To confirm the presence of amine sites over the surface, we assayed with a specific reagent used in proteins, 2,4,6-trinitrobenzenesulfonic acid solution (TNBS) measuring an absorbance band at 340 nm [22]. The results were not significantly conclusive, probably due to the low total amine concentration in the nanoparticle solution and the sensitivity of the colorimetric method.

The presence of amine groups over the nanoparticle surface was confirmed with Zeta-seizer potential measurements (PVP gold NPs signal approximately −20 and amine gold nanoparticles +17). For the linking of the different spacers, nanoparticles were redispersed in buffer phosphate 100 mM, pH 7.40, and 2–3 mg (~2–4 μmol) of the spacer arm was added in 1 mL of amine gold nanoparticles with continuous shaking during 45 min. In these conditions we had a ratio of ($-NH_2$/spacer) about 1000 times and no aggregation caused by crosslinking between two or more nanoparticles was observed. After 45 min, we added an equimolar (~2–4 μmol) amount of 3-(amine)phenyl boronic acid and allowed it to react 2–3 h. Afterwards, nanoparticles were centrifugated and washed with buffer phosphate. At this point the nanoparticle surface was modified with different spacers linked to phenyl boronic acid. It is well known that boronic acid reacts specifically with diols [23]; for this reason it can be covalently linked to cyclodextrins, as demonstrated in the different nanosensors developed with quantum Dots [24]. βCD grafting on gold nanoparticles was done by redispersing 1 mL of phenyl boronic modified nanoparticles in 1 mL of βCD 5 mM in buffer phosphate pH 7.40, and allowed to react for 3 h with continuous shaking. The centrifuge always washes and conserves the nanoparticles in buffer phosphate. The covalent bond between cyclodextrin diol and boronic acid is affected by pH (it is stable between pH 7–8). See structure synthesized, Scheme (1).

A concentrated aqueous solution of RhB (3 mg/10 mL) was stored in the refrigerator (4 °C) for a maximum of 20 days. The stability of the stock solutions was periodically checked by spectrophotometry before preparing the appropriate dilutions for fluorimetric determinations. All the experiments were done with diluted aqueous solutions of RhB in the nM range to ensure that only the monomeric species was present. All the solutions were covered with aluminum foil to protect them from light exposure. For emission and excitation fluorescence spectra, the excitation and emission bandwidths were set at 5 nm. Fluorescence emission spectra were measured with an excitation wavelength equal to the wavelength of maximum absorption. All the measurements were made at (25.0 ± 0.1) °C, with the temperature of the cell compartment controlled with a Haake K10 circulator with continuous stirring. The lifetime measurements of RhB were performed for different media (Au@spacer$_n$-βCD, only in buffer solution, free βCD, free Au NPs and a mechanical mix of free βCD and free Au NPs).

In all cases, low concentrations (approximately $3.88 \cdot 10^8$ NPs/mL, or a dilution factor of 100 of the initial gold mother solution) of gold nanoparticles were used to avoid auto-absorption (extinction coefficient lower than 0.05). The mechanical mix was done with the simple addition of nanoparticles capped with PVP 40 and βCD without adding any linker (with similar theoretical concentrations found over the total nanoparticle surface).

3. Results and discussion

3.1. Nanoparticle characterization

The particles synthesized by the classical Turkevich method were nearly monodisperse spheres and their size was easily controlled by the ratio of initial reagent concentrations. The monodisperse spherical gold nanoparticles, 40–50 nm diameter range (Fig. 1), were characterized by UV (results shown in Fig. 2).

They were easily characterized in UV due to their plasmon absorbance band centered at 540 nm for the 55.5 nm gold nanoparticles.

The surface modifications of Au NPs can be easily observed in UV. As a representative example, we show in Fig. 2 the case of Au@spacer$_9$-βCD. Here, the grafting of the different spacers and boronic linker can be seen with the presence of a band at 240–250 nm. Furthermore, the grafting of organic molecules on the surface red shift the gold plasmon band by a few nanometers caused by nanoparticle aggregation into the dispersion, as it was shown in aggregates of gold nanoparticles grafted with ADN [25]. This phenomenon was not observed for the mixing of nanoparticle, spacers and βCD not linked; and the UV of the mixing was the sum of all the components separately. We also found a third band at 650–660 nm, consistent with results reported in previous publications, where modified cyclodextrins (such as pyridylmethylamino-β-cyclodextrin) were grafted on gold nanoparticles [26]. These spectral characteristics were observed for the three types of linkers used.

As shown in Fig. 3, the gold nanoparticle plasmon has a good overlap with RhB, required for the interaction of nanoparticle plasmon with RhB excitation wavelength in the near field, and with the RhB emission wavelength in the far field. These requirements need to be complied with in order to achieve an optimal fluorophore nanoparticle plasmon coupling and the resulting MEF phenomena [27].

3.2. Effect of the cyclodextrin on rhodamine emission fluorescence by host–guest complex formation

It is known that RhB has a high cyclodextrin constant association value related to strong host–guest interaction; and moreover the RhB dye is quenched by the cyclodextrin. However, in this work, we want to explore its strong interaction and recognition as a mimetic enzymatic model linked to a metallic nanoparticle and assay to control the effect observed on fluorescence by varying the spacer lengths. As seen in Fig. 4, RhB emission in the presence of βCD (10 mM) has the quenching effect reported previously in the literature [28] (quenching effect measured is ~25%) and characteristic blue shift ($\lambda_{max.\ em.}$ 574.0 nm) as those observed for this dye in the literature [29]. Analyzing the supramolecular complex, from the interaction point of view, this host–guest

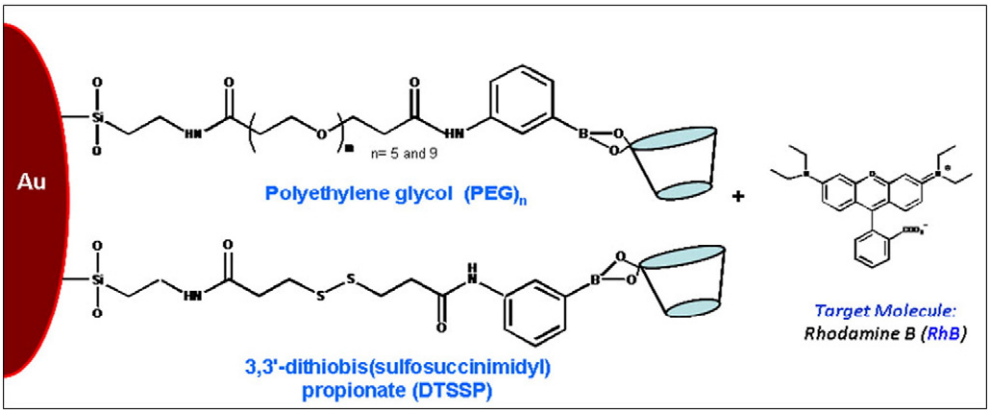

Scheme 1. Schematic representation of Au@spacer$_n$-βCD.

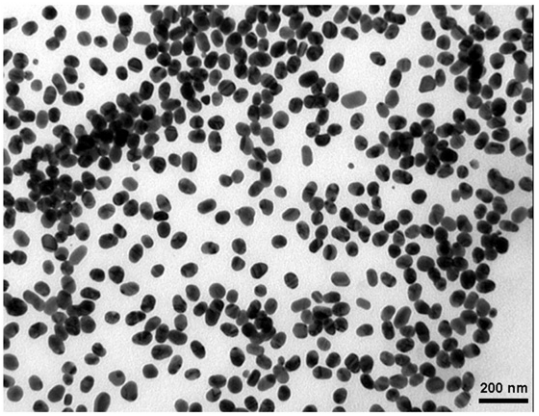

Fig. 1. TEM of gold nanoparticles synthesized by the classical Turkevich method of citrate reduction of $HAuCl_4$. Monodisperse spherical gold nanoparticles of 55.5 nm diameter were obtained.

is ideal due to the host–guest complementarity and strong association constant; but in terms of the stabilization of the excited state it has no advantages for analytical applications. For this reason it is very interesting to study the plasmonic effect on the fluorescence emission of the host–guest complex. In general, it could be observed that the effect on the quantum yields due to a plasmonic interaction is higher when the quantum yields are lower.

3.3. Effect of different spacers on rhodamine–cyclodextrin complex emission over gold nanoparticles

Specifically with nanoparticles, we studied the effect of cyclodextrin grafting with different length spacers attached to gold nanoparticles.

In each medium (Au@spacer$_n$-βCD), we monitored changes over a one-hour period in the fluorescence spectra of Au@spacer$_n$-βCD in the presence of 1.0 nM of RhB with continuous stirring. Fig. 5 shows a representative result of the spectra obtained with the spacer arms (DTSSP, 1.2 nm, $n = 5$ (BS (PEG)$_5$, 2.17 nm) and $n = 9$ (BS (PEG)$_9$, 3.58 nm) for (BS (PEG)$_9$. As can be seen, there is a 60% increase in RhB emission signal ($\lambda_{max.\ em.}$ 580.0 nm) with time, accompanied by a 6-nm blue shift in the emission peak wavelength over the first 45 min; after that, it was stabilized.

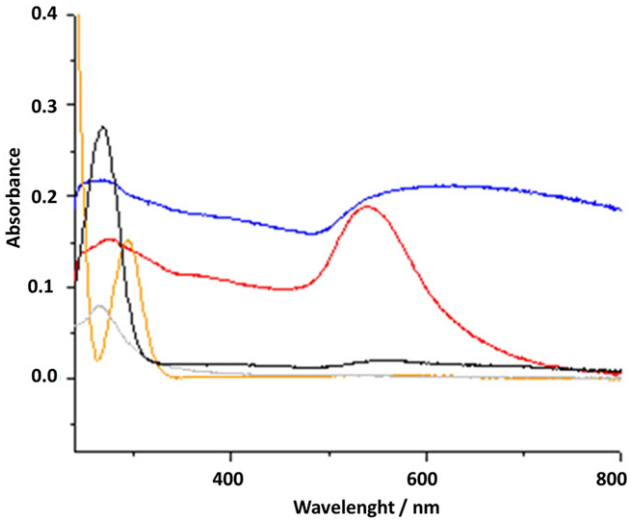

Fig. 2. UV spectra in buffer phosphate pH = 7.40: a) gold nanoparticles grafted with βCD using, as a spacer, bis-succinimide ester activated PEG (polyethylene glycol) BS (PEG)$_9$ (blue line). b) gold nanoparticles, diameter = 55.5 nm (red line). c) Spacer BS(PEG)$_9$ (black line). d) β-cyclodextrin spectra (gray line). e) 3-amine phenyl boronic acid linker (orange line).

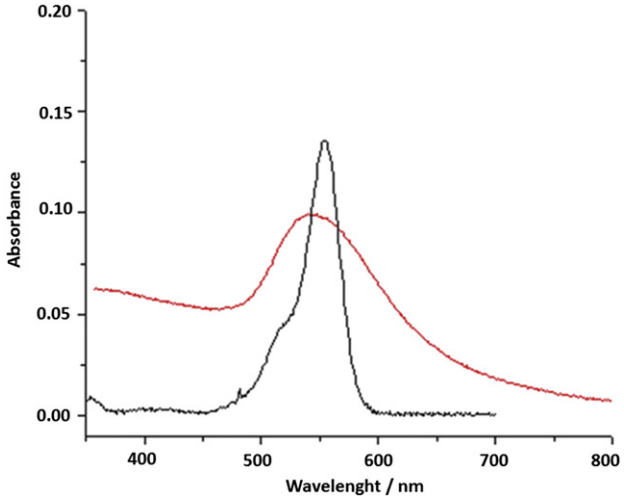

Fig. 3. UV spectra of gold nanoparticles (red line) and rhodamine B (black line). Experimental conditions: [Au NPs] = $1.29 \cdot 10^8$ and [RhB] = 2.5 μM in buffer phosphate pH = 7.40.

The enhanced fluorescence can be attributed to an interaction with a supramolecular recognition of the guest (RhB), and due to the proximity of the fluorophore with the metallic nanoparticle an increase of the absorption at the maximal absorption wavelength of the fluorophore in the near field is generated. This phenomenon is one of the most important factors related to MEF.

Yet with the first supramolecular recognition between RhB and βCD a quenching effect is observed [30] at low concentration (~10^{-8} M), in presence of Au@spacer$_n$-βCD, the host–guest recognition allows encapsulation and approaching of the dye to the metallic surface causing metal enhanced fluorescence (MEF). It is well known that MEF effect is related to the distance between metal surface and fluorophore, a dependence shown by different studies into metal–fluorophore interaction [31]. As seen in Fig. 6, a tendency is found in the values obtained with the maximal signal stabilized after 50 min and the spacer length.

Table 1 displays increases of 25%, 47% and 59% for spacers DTSSP and BS (PEG)$_n$ ($n = 5$ and 9) respectively, showing the tendency for increase with the longer spacer arm length. This tendency is explained by the

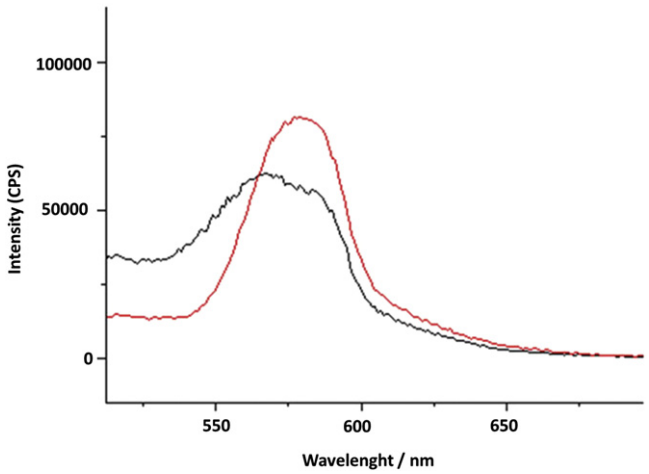

Fig. 4. Fluorescence spectra of rhodamine B: in buffer phosphate pH = 7.40 (red line) ($\lambda_{max.\ em.}$ = 580.0 nm), and in the presence of βCD (black line) ($\lambda_{max.\ em.}$ = 574.0 nm). Rhodamine B and βCD concentrations were 1.0 nM and 10.0 mM respectively.

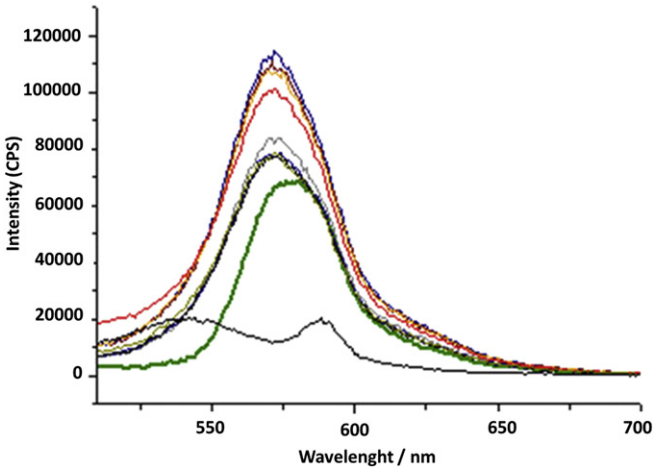

Fig. 5. Fluorescence spectra of rhodamine B in buffer phosphate pH = 7.40 (green line) ($\lambda_{max.\ em.}$ = 580.0 nm), and in the presence of Au@spacer$_n$-βCD with n = 9 (BS (PEG)$_9$, 3.58 nm in a period of 1 h (blue line corresponds to 1 h). Nanoparticle blank, Au@spacer$_n$-βCD (black line).

dependence of the maximal electromagnetic field intensity generated with the distance in the near field.

The increases observed are lower than other MEF effects from other nanostructures reported in the literature with core–shell nanoparticles; however, these cases show a higher inter shell concentration of fluorophores in the range of μM–mM, compared with the nM βCD concentration grafted over total nanoparticle concentration.

3.4. Effect of the pH on the fluorescence emission of the fluorescent complex

The fluorescence intensity of the RhB in the presence of the nanosensor was diminished to the RhB free value in solution at the 1 nM level in the pH range, 8.5 < pH < 5.5, caused by the non formation of the boronic acid linkages with diols in these conditions. At neutral pH due to that the boronic acid is a weak Lewis acid the trigonal form of the acid exists and this is the specie responsible of the bond formation with

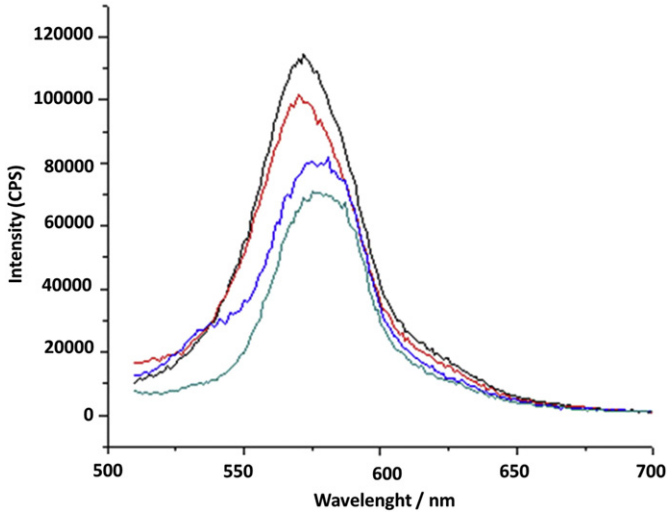

Fig. 6. Fluorescence spectra of rhodamine B in buffer phosphate pH = 7.40 (green line) ($\lambda_{max.\ em.}$ = 580.0 nm), and in the presence of Au@spacer$_n$-βCD with different spacers: DTSSP, 1.2 nm (blue line), n = 5 (BS (PEG)$_5$, 2.17 nm (red line) and n = 9 (BS (PEG)$_9$, 3.58 nm (black line).

Table 1

Spacer	Length (Å)[a]	Total length (Å)[b]	%(I/I$_0$)[c]
DTSSP	12.0	~30	25
BS (PEG)$_n$ (n = 5)	21.7	~40	47
BS (PEG)$_n$ (n = 9)	35.8	~54	59

Percentage of rhodamine B fluorescence emission increment in the presence of nanosensor Au@spacer$_n$-βCD with a specific spacer arm (%(I/I$_0$)).

[a] Spacer arm length.

[b] The total length takes into account cyclodextrin dimension of 1.8 nm.

[c] I/I$_o$ is the maximum signal intensity ratio between RhB in the presence of Au@spacer$_n$-βCD and RhB free in buffer.

diols [32]. Moreover the association constant of the complex RhB–βCD is high (7.10^3 M^{-1}) at neutral pHs due to their aromatic moiety complexation that occurs by hydrophobic effect enhanced by hydrogen bonds from the deprotonated carboxylic acid and the CD hydroxyls groups [33].

3.5. Switch on/off enhanced fluorescence control and βCD–RhB complex delivery

In the presence of the cyclodextrin DTSSP linking, we were also able to reduce the disulfide covalent bond with a specific reducing agent, DL-1,4-dihiothretol (DTT), for complex delivery. Hence, we can control the enhanced fluorescence effect of this nanosupramolecular system using reducing and oxidant agents, giving the time needed for each reaction (Scheme 2).

In Fig. 7, we can see the increase in fluorescence with time (blue line to red line). After signal stabilization, DTT reducing agent was added. Following a few minutes, the signal was reduced to the initial RhB fluorescence (red line to green line). Thus, complex delivery was carried out, and the free βCD complex not attached to the metallic nanoparticle (at nanomolar levels) showed no increase in fluorescence.

This reaction is particularly useful for us not only to simulate an enzymatic activity with complex delivery over a nanoparticle surface, but also as a tool to confirm different events. First, all the reaction steps and βCD grafting can be controlled; second, we can control the enhanced fluorescence effect; and third we can confirm the importance of the supramolecular host–guest interaction and recognition at nanolevels only over a metallic nanoparticle surface. These observations have synthetic and analytical applications in future works for biosensor designs with fluorescent methods.

3.6. Fluorescence lifetime measurements

In order to understand the photo-physics of RhB and to obtain more information on the micro environmental changes around the fluorophore interacting with the different media, we measured fluorescence-lifetime decays in the conditions described before. As you can see in Fig. (8), decay curves show that there is a shortening of lifetime in RhB dye in the presence of the nanosensor as compared with the free RhB in buffer phosphate and also in the presence of free gold nanoparticles (without βCD grafting). Table (2) show all the results obtained. This fluorescence-lifetime decay shortening is explained in MEF by a higher occupation of the upper excited levels based on higher excitation intensity.

The lifetime value obtained for RhB in buffer was 1.6 ns, in agreement with the results reported previously (1.6 ns) [34] and (1.7 ns) [35]. To evaluate distance effect on lifetime value averages, we chose DTSSP (1.20 nm) and BS (PEG)$_9$ (3.58 nm) spacers. The values obtained for both spacers were similar to and smaller than 50% compared with RhB free in buffer, as seen in Table 2. Although lifetime value averages in the presence of both spacers are lower than those obtained with RhB free in buffer, they showed no decrease between the two spacers. Moreover, in the presence of the nanosensor modified with the DTSSP

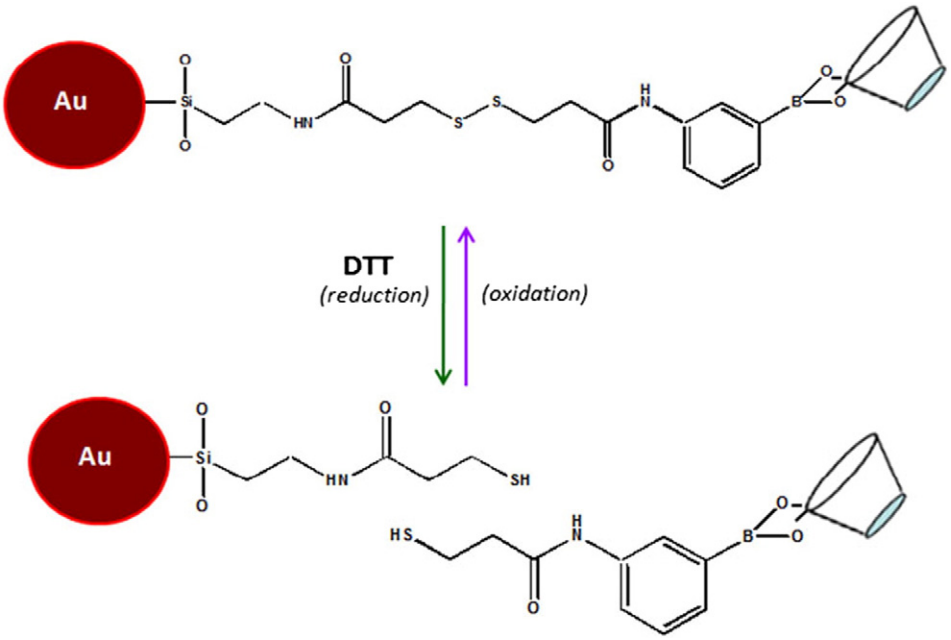

Scheme 2. Reduction reaction of disulfide covalent bond with DL-1,4-dihiothretol (DTT) for βCD complex delivery.

spacer arm, the RhB emission measured showed a lifetime shortening that it was recovered after addition of DDT reductant agent as it can see in Fig. 8 and Table 2.

Considering the nanoarchitecture and distance effect on the emission with the different spacer's lengths, we have to take into account that linkers are flexible polar hydro-carbonated chains with a cyclodextrin linked to the end of the molecular spacer, as micelles surrounding nanoparticle surface. Yet, this nanoarchitecture will allow not only host–guest recognition; depending on the guest polarity may be the dye could also interact by noncovalent interaction with carboxylic groups or mercaptophenylboronic acid not substituted between two cyclodextrins linked. However, as we can see in Table 2, when the mechanical mix of gold nanoparticles (without amine groups) was measured with DTSSP, βCD and RhB, the average lifetime value measured was that obtained for RhB free in buffer. This result shows that the βCD–RhB complex linked to the nanoparticle surface is required to obtain a decrease in lifetime as found in the presence of Au@spacer$_n$-βCD with both spacer arms. Viger et al. (supporting information) [36] also worked with fluorescent core–shell nanoparticles. They measured differences of lifetime value averages of around 0.25 ns between spacer thickness of 7 (0.159 ns) and 13 nm (0.388 ns). For this reason, in the nanosensor synthesized, the difference between the distances of the spacer arms is not significant enough to obtain different lifetime decay values. Yet, in both cases we obtained a decrease in RhB lifetime values only in the presence of the nanosensor [37,38].

4. Conclusion

A PEG-βCD gold nanoparticle capped was developed using different PEG chain lengths. In this way, it was found that the optimal PEG length to attain the best rhodamine B fluorescence emission enhancement was around 4–5 nm with a 60% increase. At shorter PEG lengths, 1.2 and

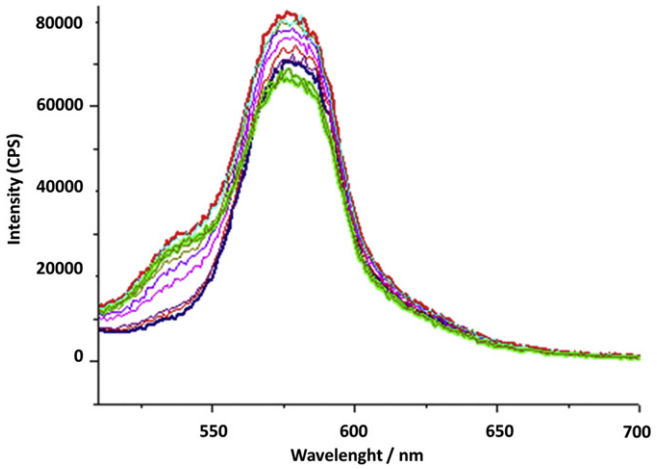

Fig. 7. Fluorescence spectra of rhodamine B in the presence of Au@spacer$_n$-βCD (spacers: DTSSP, 1.2 nm) a) at time = 0 (blue line) b) 1 h period (red line) c) after 10 min of adding DTT (green line).

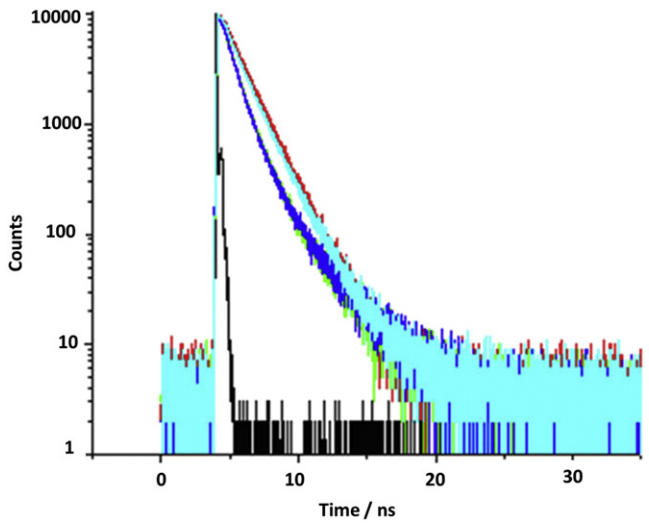

Fig. 8. Rhodamine lifetime decays: rhodamine B free in buffer (red line), and in the presence of Au@spacer$_n$-βCD with different spacers: $n = 9$ (BS (PEG)$_9$, 3.58 nm (blue line); DTSSP, 1.2 nm (green line) and DTSSP spacer arm with the addition of DTT reducing agent (turquoise line).

Table 2

Sample[a]	τ_1 (ns)[b]	A_1%[b]	τ_2(ns)[b]	A_2%[b]	C2[c]	τ_{av} (ns)[d]
RhB	1.589 (0.009)	100	– –	–	1.016	1.589
NPs with BS $(PEG)_9$ spacer + RhB	0.892 (0.012)	89	2.331 (0.051)	11	1.69	1.050
NPs withDTSSPspacer + RhB	0.872 (0.012)	90.5	2.504 (0.057)	9.5	1.855	1.026
NPs withDTSSP spacer + DTT + RhB	1.092 (0.021)	62	1.928 (0.024)	38	1.686	1.510
Mech. Mix. Au NPs + DTSSP + CD + RhB	1.595 (0.013)	100	– – –	–	1.989	1.595

Rhodamine B lifetime values in different media.

[a] RhB 2.9 nM in the presence of the different media.

[b] τ, A_1, A_2 are lifetime and amplitude values for the first and second fitting components respectively.

[c] C2 is the quality of fit parameter.

[d] τ_{av} is the lifetime value average.

2.17 nm, it was observed smaller increases of 25 and 47% respectively. Even at these shorter spacer distances it was possible to overcome the quenching effect of the RhB by the βCD host–guest complex. Fluorescence lifetime decays showed a 50% decrease in the presence of the nanosensor, characteristic of MEF effect, compared with RhB free in solution. In addition, it was possible to control the enhanced fluorescence emission by the reduction of a di-thiane linker and delivery of rhodamine βCD complex. After cleavage of di-thiane linkers, the enhanced fluorescence emission was quenched and the lifetime value mean of RhB was increased, recovering the standard value of RhB free in solution. By this manner it was demonstrated the sensitivity of the gold core on the emission signal, and the supramolecular interaction in order to form a host–guest complex at a given distance from the metallic surface of the nanoparticle.

Thus, the design proposed demonstrates the concept for supramolecular nanostructures, allowing the detection of fluorescent organic molecules and a controlled delivery of a complexed drug at the right place and time. Moreover, even if molecules are not fluorescent, other methodological detection strategies could be applied to the same nanosensor architecture.

Acknowledgments

The acknowledgments are for the different grants to accomplish this work. Moreover, we acknowledge Professor Denis Boudreau for the postdoctoral position and the Département de chimie and Centre d'optique, photonique et laser, Québec, Canada. We also acknowledge CONICET (Consejo Nacional de Investigaciones Científicas y Tecnológicas de Argentina), the National Research Council of Argentine for the position as researcher at the INFIQC (Instituto de Investigaciones en Fisicoquímica de Córdoba, Argentina), the Institute of Physicochemical Research of Cordoba, Argentine.

References

[1] E.V. Anslyn, Supramolecular analytical chemistry, J. Org. Chem. 72 (2007) 687–699.
[2] D.C. Gutsche, Calixarenes, Monographs in Supramolecular Chemistry, 2nd ed., Series Editor: J. Fraser Stoddart, vol. 1, RSC, 1998.
[3] J. Lagona, P. Mukhopadhyay, S. Chakrabarti, L. Isaacs, The cucurbit[n]uril family, Angew. Chem. Int. Ed. 44 (2005) 4844–4847.
[4] M.L. Bender, M. Komiyama, Cyclodextrin Chemistry, Springer-Verlag, Berlin, Heidelberg, 1978.
[5] Y. Liu, Y. Chen, S.X. Liu, X.D. Guan, T. Wada, Y. Inoue, Unique fluorescence behavior of rhodamine B upon inclusion complexation with novel bis(β-cyclodextrin-6-yl) 2,2′-bipyridine-4,4′-dicarboxylate, Org. Lett. 3 (2001) 1657–1660.
[6] D. Yuan, K. Koga, Y. Kourogi, K. Fujita, Synthesis of fullerene-cyclodextrin conjugates, Tetrahedron Lett. 42 (2001) 6727–6729.
[7] M.C. Marchi, S.A. Bilmes, G.M. Bilmes, Photophysics of rhodamine B interacting with silver spheroids, J. Colloid Interface Sci. 218 (1999) 112–117.
[8] Z. Yu, M. Yu, Z. Zhang, G. Hong, Q. Xiong, Bovine serum albumin nanoparticles as controlled release carrier for local drug delivery to the inner ear, Nanoscale Res. Lett. 9 (2014) 343 (1–7).
[9] M. Ohtsu, K. Kobayashi, T. Kawazoe, S. Sangu, T. Yatsui, Nanophotonics: design, fabrication, and operation of nanometric devices using optical near fields, IEEE J. Sel. Top. Quant. Electron. 8 (2002) 839–862.
[10] J.R. Lackowicz, Radiative decay engineering: metal enhanced fluorescence and plasmon emission, Anal. Biochem. 337 (2005) 171–194.
[11] M. Lessard-Viger, M. Rioux, L. Rainville, D. Boudreau, FRET enhancement in core shell nanoparticles, Nano Letters 9 (8) (2008) 3066–30718.
[12] K. Ray, M.H. Chowdhury, H. Szmacinski, J.R. Lakowicz, Metal-enhanced intrinsic fluorescence of proteins on silver nanostructured surfaces toward label-free detection, J. Phys. Chem. C 46 (112) (2008) 17957–17963.
[13] M. Lessard-Viger, D. Brouard, D. Boudreau, Plasmon enhanced energy transfer from a conjugated polymer to fluorescent core shell nanoparticles: a photophysical study, J. Phys. Chem. C 115 (7) (2011) 2974–2981.
[14] J.M. Campiña, A. Martins, F. Silva, Immobilization of β-cyclodextrin on gold surfaces by chemical derivatization of an 11-amino-1-undecanthiol self-assembled monolayer, Electrochim. Acta 18 (2009) 90–103.
[15] N. Zhang, Y. Liu, L. Tong, K. Xu, L. Zhuo, B. Tang, A novel assembly of Au NPs–β-CDs–FL for the fluorescent probing of cholesterol and its application in blood serum, Analyst 133 (2008) 1176–1181.
[16] X. Chen, S.G. Parker, G. Zou, W. Su, Q. Zhang, ß-Cyclodextrin-functionalized silver nanoparticles for the naked eye detection of aromatic isomers, ACS Nano 4 (2010) 6387–6394.
[17] Y. Wu, F. Zuo, Z. Zheng, X. Ding, Y. Peng, A novel approach to molecular recognition surface of magnetic nanoparticles based on host–guest effect, Nanoscale Res. Lett. 4 (2009) 738–747.
[18] S. Liu, Y. Han, R. Qiao, J. Zeng, Q. Jia, Y. Wang, M. Gao, Investigations on the interactions between plasma proteins and magnetic iron oxide nanoparticles with different surface modifications, J. Phys. Chem. C 114 (2010) 21270–21276.
[19] M.E. Davis, J.E. Zuckerman, C.H.J. Choi, Evidence of RNAi in humans from systemically administered siRNA via targeted nanoparticles, Nature 464 (2010) 1067–1070.
[20] E.S. Gil, J. Li, H. Xiao, T.L. Lowe, Quaternary ammonium beta-cyclodextrin nanoparticles for enhancing doxorubicin permeability across the in vitro blood–brain barrier, Biomacromolecules 10 (2009) 505–516.
[21] J.R. Lakowicz, Radiative decay engineering 5: metal-enhanced fluorescence and plasmon emission, Anal. Biochem. 337 (2005) 171–194.
[22] G.T. Hermanson, Bioconjugate Techniques, second ed. Elsevier, 2008.
[23] C. Cannizzo, S. Amigoni-Gerbier, C. Larpent, Boronic acid funcionalized nanoparticles: synthesis by microemulsion polymerization and applications as a reusable optical nanosensor for carbohydrates, Polymer 46 (2005) 1269–1276.
[24] R. Freeman, T. Finder, L. Bahshi, I. Willner, β-Cyclodextrin-modified CdSe/ZnS quantum dots for sensing and chiroselective analysis, Nano Letters 9 (2009) 2073–2076.
[25] J.J. Stohoff, A.A. Lazarides, R.C. Mucic, C.A. Mirkin, R.L. Letsinger, G.C. Schatz, What controls the optical properties of DNA-linked gold nanoparticle assemblies? J, Am. Chem. Soc. 122 (2000) 4640–4650.
[26] Q. Zeng, R. Marthi, A. McNally, C. Dickinson, T.E. Keyes, R.J. Foster, Host–guest directed assembly of gold nanoparticle arrays, Langmuir 26 (2) (2010) 1325–1333.
[27] C.D. Geddes, Metal Enhanced Fluorescence, Wiley, 2010.
[28] I.R. Politzer, K.T. Crago, T. Hampton, J. Joshep, Effect of b-cyclodextrin on the fluorescence, absorption and lasing of rhodamine 6G, rhodamine B and fluorescein disodium salt in aqueous solutions, Chem. Phys. Lett. 159 (1989) 258–262.
[29] I. Degani, I. Willner, Lasing of rhodamine bin aqueous solution containing β-cyclodextrins, Chem. Phys. Lett. 104 (5) (1984) 496–499.
[30] I.R. Politzer, K.T. Crago, T. Hampton, J. Joshep, Effect of β-cyclodextrin on the fluorescence, absorption and lasing of rhodamine 6G, rhodamine B and fluorescein disodium salt in aqueous solutions, Chem. Phys. Lett. 159 (1989) 258–262.
[31] A. Wokaun, H.P. Lutz, A.P. King, U.P. Wild, R.R. Ernst, Energy transfer in surface enhanced luminescence, J. Chem. Phys. 79 (1983) 509–514.
[32] H.S. Mader, O.S. Wolfbeis, Boronic acid based probes for microdetermination of saccharides and glycosylated biomolecules, Microsc. Acta 162 (2008) 1–34.
[33] J.A.B. Ferreira, S.M.B. Costa, Nonradiative decay in rhodamines: role of 1:1 and 1:2 molecular complextion with βcyclodextrin, J. Photochem. Photobiol. A Chem 173 (2005) 309–318.

[34] M.J. Snare, F.E. Treloar, K.P. Ghiggino, P.J. Thistlethwaite, The photophysics of rhodamine B, J. Photochem. 18 (1982) 335–346.
[35] F. Lopez, P. Ruiz Ojeda, I. Lopez Arbeloa, Flourescence self-quenching of the molecular forms of rhodamine B in aqueous and ethanolic solutions, J. Lumin. 44 (1989) 105–112.
[36] M. Lessard-Viger, M. Rioux, L. Rainville, D. Boudreau, FRET enhancement in multilayer Core–Shell nanoparticles, Nano Letters 9 (2009) 3066–3071.
[37] J.R. Lackowicz, Radiative decay engineering: biophysical and biomedical applications, Anal. Biochem. 298 (2001) 1–24.
[38] C.D. Geddes, J.R. Lackowicz, Editorial: metal-enhanced fluorescence, J. Fluoresc. 12 (2) (2002) 121–129.